Microsc. Microanal. 19, S5, 29–32, 2013
doi:10.1017/S1431927613012270

Characterization of Sc_2O_3&CeO_2-Stabilized ZrO_2 Powders Via Co-Precipitation or Hydrothermal Synthesis

Justyna Grzonka,[1,*] Victor Vereshchak,[2] Oleksiy Shevchenko,[3] Oleksandr Vasylyev,[3] and Krzysztof J. Kurzydłowski[1]

[1]*Faculty of Materials Science and Engineering, Warsaw University of Technology, 02-507 Warsaw, Poland*
[2]*Laboratory for Chemistry & Technology of Powder Materials, Ukrainian State University of Chemical Engineering, Dnipropetrovs'k, 49005, Ukraine*
[3]*Frantcevych Institute for Problems of Materials Science, National Academy of Sciences of Ukraine, Kyiv 03680, Ukraine*

Abstract: As the presence of Sc_2O_3 and CeO_2 is known to largely enhance the ionic conductivity in the temperature range of 600–800°C, compared with the conventional yttria-stabilized ZrO_2, Sc_2O_3&CeO_2-stabilized ZrO_2 provide its applicability as electrolytes in solid oxide fuel cells. The current study introduces the methodology to synthesize Sc_2O_3&CeO_2-stabilized ZrO_2 powders by using co-precipitation technique or high-temperature hydrothermal reaction, and further describes the structural characterization of the zirconia powders synthesized by the above-mentioned two methods. The co-precipitation technique was found to allow obtaining powders of cubic phase, whereas high-temperature hydrothermal synthesis results in the presence of a monoclinic phase as well. The scanning transmission electron microscope observations also confirm that the size of the synthesized ZrO_2 powders in this study is found to be much smaller than that of commercially available powders.

Key words: Scandia ceria co-stabilized zirconia powders, nanocrystalline materials, grain size, solid oxide fuel cells, scanning transmission electron microscopy

Introduction

Stabilized ZrO_2-based oxides are widely used now as an electrolyte in solid oxide fuel cells (SOFC) because of their high oxide ion conductivity and good chemical stability under SOFC operation conditions. One of the most popular oxides used as a stabilizer in ZrO_2 is Y_2O_3, which guarantees good mechanical, chemical, and electrical properties. The yttria-stabilized zirconium oxides known as the Nernst's mass are used as a solid electrolyte components in SOFC devices operating above 800°C (Baur & Preis, 1937). The ionic conductivity of ceramic solid electrolytes increases with higher temperatures. However, by decreasing operating temperatures it is possible to improve their stability, reliability, and material cost. Numerous observations showed that the highest oxide ionic conductivity at intermediate temperatures (600–800°C) in ZrO_2-based systems is achieved by stabilizing with Sc_2O_3 (Kilner & Brook, 1982).

The drawback of Scandia-stabilized ZrO_2 is that around temperature 650°C there is a phase transition from cubic to rhombohedral resulting in reduction of the conductivity. Various attempts have been made to stabilize the c-phase by substituting the 1 mol% of Sc_2O_3 with other oxides such as Gd_2O_3, Y_2O_3, Bi_2O_3, CeO_2, Al_2O_3, and TiO_2. Among various co-doped oxides, the highest ionic conductivity at 600°C was measured for CeO_2 and 10 mol% Sc_2O_3–1 mol% CeO_2–89 mol% ZrO_2 (10Sc1CeSZ) was proposed for SOFC application (Haering et al., 2005).

*Corresponding author. E-mail: j.grzonka@inmat.pw.edu.pl

The 10Sc1CeSZ powders could be obtained through different techniques, including co-precipitation (Lei & Zhu, 2005), using citrate (Okamoto et al., 2005), polymeric precursor (Tu et al., 2011), spray drying (Tietz et al., 1997), combustion (Lei et al., 2006), and sol-gel (Mizutani et al., 1994). Among them, co-precipitation and high-temperature hydrothermal routes are the most widely used on industrial scale. The aim of the present paper was to study the structural features of powders produced by co-precipitation and hydrothermal techniques, and compare them with their commercial counterparts.

Materials and Methods

The zirconia powders stabilized with scandium and cerium oxides (10Sc1CeSZ: 10 mol% Sc_2O_3–1 mol% CeO_2–89 mol% ZrO_2) were obtained through co-precipitation technique and high-temperature hydrothermal synthesis. Co-precipitated 10Sc1CeSZ powder was produced at Vilnohirsk Mining & Metallurgical Plant (VMMP), Ukraine. The $ZrOCl_2 \cdot 8H_2O$ and Sc_2O_3, commercially available at VMMP from a natural Ukrainian source, were used for synthesis of the powders. The initial solution was prepared by dissolving $ZrOCl_2 \cdot 8H_2O$ in distilled water at 60°C with appropriate amount of Sc_2O_3 dissolved under stirring conditions. After addition of Sc_2O_3, 1 mol% of Ce^{4+} in the form of $CeCl_4$ was added and the resulting solution was left for 24 h at room temperature.

The process of co-precipitation was performed at pH 9.5 by adjusting the solution basicity using NH_4OH. The precipitates were washed with distilled water to remove Cl^- and

Table 1. The Size of Agglomerates and Particles of 10Sc1CeSZ Powders.

No	Powder	Laser Scattering Particle Size Distribution Analyzer	XRD Analysis—Williamson–Hall Method	Image Analysis—Micro Meter Program
1	10Sc1CeSZ (DKKK)	1.4 μm ($\pm$0.4 μm)	73 nm	83 nm ($\pm$20 nm)
2	10Sc1CeSZ (Praxair)	1.3 μm ($\pm$0.3 μm)	64 nm	141 nm ($\pm$60 nm)
3	10Sc1CeSZ (co-precipitation I)	2.3 μm ($\pm$0.2 μm)	12 nm	11 nm ($\pm$2 nm)
4	10Sc1CeSZ (co-precipitation II)	2.0 μm ($\pm$0.2 μm)	11 nm	13 nm ($\pm$2 nm)
5	10Sc1CeSZ (hydrothermal)	3.3 μm ($\pm$0.3 μm)	—	13 nm ($\pm$2 nm)

XRD, X-ray diffraction; DKKK, Daiichi Kigenso Kagaku Kogyo Co.

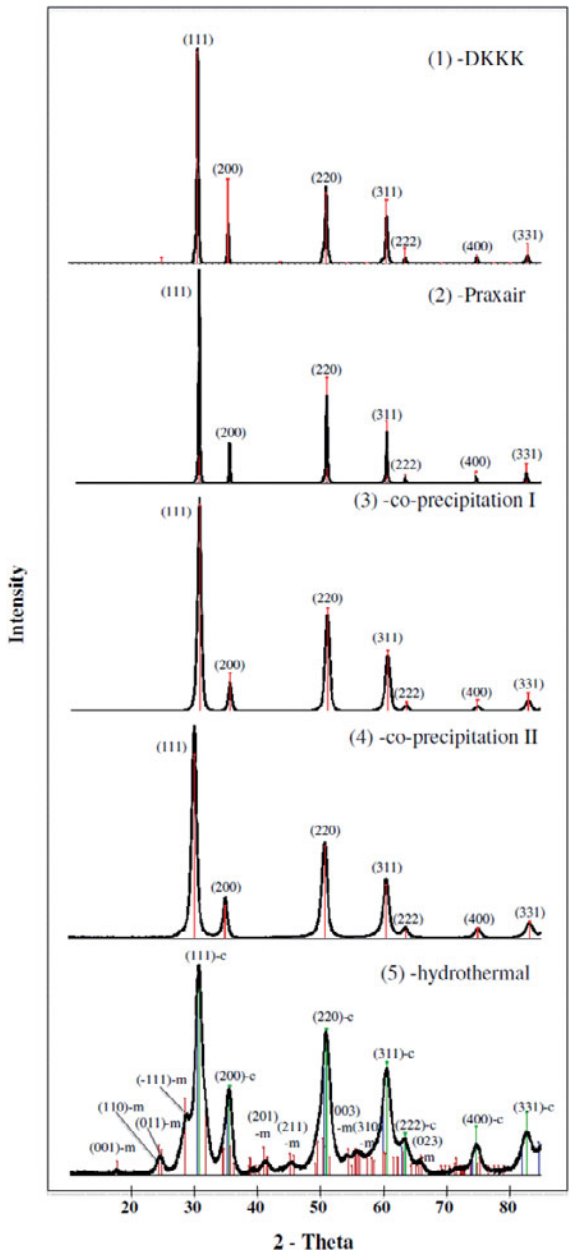

Figure 1. X-ray diffraction patterns of (1) Daiichi Kigenso Kagaku Kogyo Co. (DKKK), (2) Praxair, (3) co-precipitation I, (4) co-precipitation II, and (5) hydrothermal powders.c, cubic phase; m, monoclinic phase.

NH_4^+ ions. In order to avoid formation of the aggregates, they were dried by azeotropic distillation with butyl alcohol followed by sintering of the xerogels at 700–850°C in air. Two types of powders were produced called co-precipitation I and co-precipitation II. They differed by the water solutions used during production process, for co-precipitation I it was 0.1 mol/L $ZrClO_4$ and for co-precipitation II it was 1.0 mol/L $ZrClO_4$.

The preparation of high-temperature hydrothermal 10Sc1CeSZ powder consisted of a few steps. First, monoclinic zirconia (M-ZrO_2) suspension was produced by hydrothermal decomposition of $ZrOCl_2 \cdot 8H_2O$ water solution up to 190°C according to the following reaction:

$$ZrOCl_2 + nH_2O \rightarrow ZrO_2 \downarrow + nH_2O + nHCl.$$

After that, the Cl^- ions were washed out from M-ZrO_2 suspension. The mixture of nanosized M-ZrO_2 suspension and $Sc(NO_3)_3 \cdot 4H_2O$ and $Ce(NO_3)_3 \cdot 6H_2O$ salts were mixed in planetary mill, in which, after mechanical and chemical treatments, Sc_2O_3 and CeO_2 were deposited on ZrO_2 nanoparticles. The new suspension was dried at 90°C, heated at 500°C, milled in isopropyl alcohol, dried at 90°C again, and annealed at 600–700°C for 4 h. The applied heat treatment results in the mechanically activated diffusion of Sc and Ce into monoclinic ZrO_2 that transforms it into cubic phase. Finally, the nanosized powder of 10Sc1CeSZ composition was obtained, which is referred to as hydrothermal in the further text.

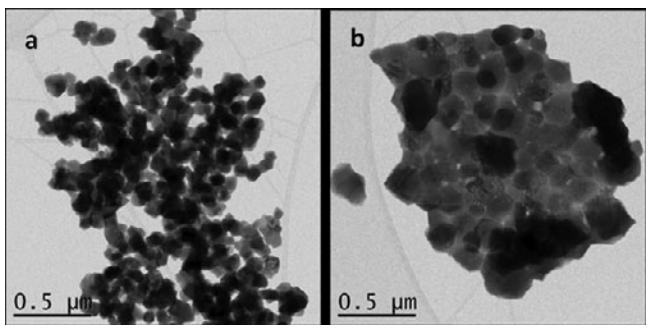

Figure 2. The bright-field scanning transmission electron microscope images of Daiichi Kigenso Kagaku Kogyo Co. (**a**) and Praxair (**b**) powders.

https://doi.org/10.1017/S1431927613012270 Published online by Cambridge University Press

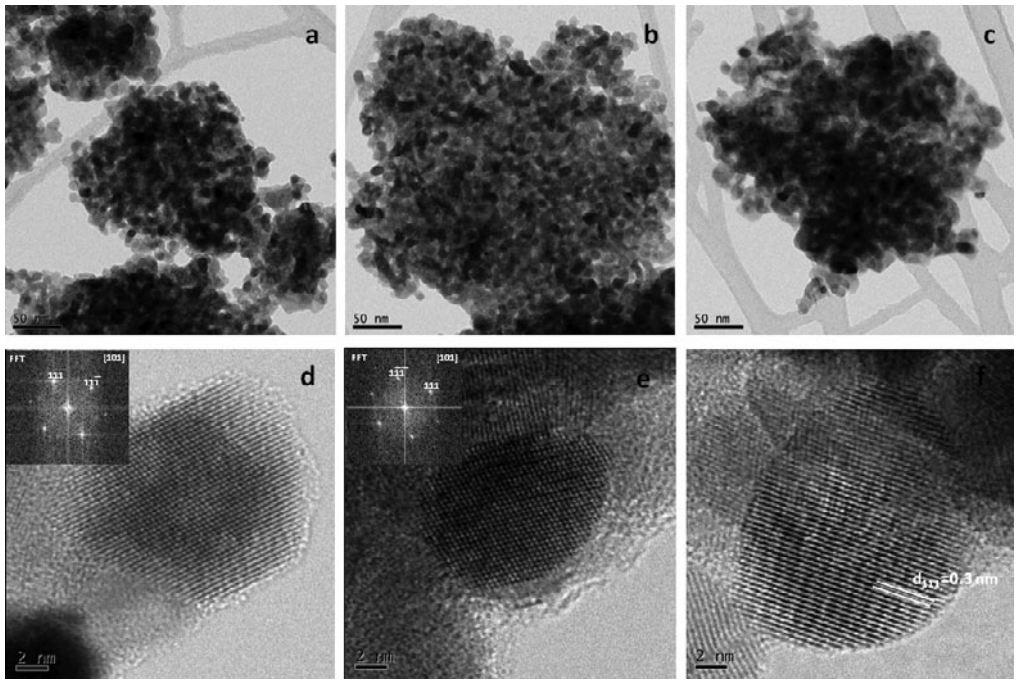

Figure 3. The bright-field scanning transmission electron microscope (STEM) (**a–c**) and high-resolution STEM (**d–f**) images of 10Sc1CeSZ powders prepared with co-precipitation I (**a**, **d**), co-precipitation II (**b**, **e**), and hydrothermal (**c**, **f**) techniques.

Properties of the obtained powders were compared against the properties of two commercial powders manufactured by Daiichi Kigenso Kagaku Kogyo Co. (DKKK), Japan, and Praxair Surface Technologies, USA, by co-precipitation and spray pyrolysis techniques, respectively. The list of the parameters used to characterize the powders is presented in Table 1.

The structure characterization of 10Sc1CeSZ powders was carried out with high-resolution scanning transmission electron microscope (STEM, Hitachi HD-2700, 200 kV, C_s corrected) with energy-dispersive X-ray spectrometer.

The X-ray diffraction (XRD) experiments were performed using Philips PW 1830 diffractometer for angle range 2Θ from 20 to 80°. The X-ray and electron diffractions were used to identify the phases. The size of grains was calculated by the Williamson–Hall method from XRD spectra and by image analyses, using the dedicated MicroMeter computer software. For image analyses, the randomly selected five high-resolution images were used for each powder. The size of powder agglomerates was estimated with a laser scattering analyzer Horiba LA-950.

Results

The results of XRD analyses are presented in Figure 1. The diffraction patterns reveal the presence of cubic phase in all powders. More detailed investigations of the hydrothermal powder show that it contains the monoclinic phase as well (Fig. 1). The XRD reveals that commercial powders have narrow peaks, indicating larger crystallites, whereas wide peaks for the powders prepared by co-precipitation and high-temperature hydrothermal techniques suggest the presence of fine crystallites.

The results of size estimate via the Williamson–Hall method (see Table 1) show that size of 10Sc1CeSZ DKKK and Praxair powders are similar and equal to 73 and 64 nm, respectively. The size of the crystallites of the co-precipitated powders was estimated at 12 and 11 nm. With respect to the size of the hydrothermal powder, application of the Williamson–Hall method was not possible because of the co-existence of the monoclinic phase and cubic phase, the peak positions of which are overlapped.

The microstructure characterization performed for commercial DKKK and Praxair powders are illustrated in Figure 2. The images shown in this figure show particles of these two powders in the diffraction contrast (bright field). One can observe that DKKK powder agglomerates, whereas Praxair powder particle resemble platelets typical for sintered ceramics containing domains and well-faceted surfaces.

Observations performed on the co-precipitation I, co-precipitation II, and hydrothermal powders show the heavy agglomeration, which is connected with the nanometer size of the particles (Figs. 3a–3c). The small size of particles called for high-resolution STEM (HR STEM) observations presented in Figure 3 together with fast Fourier transformation. The amorphous contaminations coming from the production process are also visible in HR STEM images (Figs. 3d–3f).

The HR STEM images were analyzed with the MicroMeter software. The size of particles for commercial powders determined with this method was found to be equal to

https://doi.org/10.1017/S1431927613012270 Published online by Cambridge University Press

83 nm (±20 nm) and 141 nm (±60 nm) for DKKK and Praxair powders, respectively. These figures are somewhat higher than the estimates based on XRD results, indicating that some particles might have multicrystal structure. The size of particles for the original powders investigated in this study is similar; for co-precipitation I powder it is 11 nm (±2 nm), whereas for co-precipitation II and hydrothermal powders they are 13 nm (±2 nm), as shown in Table 1. This means that the new powders have nearly order of magnitude lower size of particles, which are truly in nanorange.

The size of agglomerates was estimated with a laser scattering analyzer. The results are presented in Table 1. The largest agglomerates are about 3.3 μm (±0.3 μm). They were observed in 10Sc1CeSZ powder prepared by hydrothermal technique. The smallest aggregates were observed in commercial powders—1.4 μm (±0.4 μm) and 1.3 μm (±0.3 μm).

Discussion and Summary of the Results

The XRD analyses performed on all the powders investigated in this study show that they predominantly have a cubic structure. The presence of small amounts of monoclinic phase in hydrothermal powder reported here can be related to the sample preparation procedure. A full transition of monoclinic to cubic phase during heat treatment is very unlikely to occur.

The comparison of the results obtained from XRD spectra with the Williamson–Hall method and image analyses show that these two methods yield comparable figures. A significant difference is only encountered in the case of the Praxair powder where the particle size is more than twice bigger for image analysis method. This might be caused by multicrystal character of some of the particles.

The performed analyses show that the powders except the hydrothermal powder have the cubic structure, which is demanded for SOFC. The size of co-precipitation or hydrothermal particle powders is about 12 nm, which results in their higher agglomeration than the commercial ones.

References

Baur, E. & Preis, H. (1937). Über Brennstoff-ketten mit Festleitern. *Zeitschrift für Elektrochemie* **43**, 727–732.

Haering, C., Roosen, A., Schichl, H. & Schnöller, M. (2005). Degradation of the electrical conductivity in stabilized zirconia system. Part II: Scandia-stabilized zirconia. *Solid State Ionics* **176**, 261–268.

Kilner, J.A. & Brook, R.J. (1982). A study of oxygen ion conductivity in doped nonstoichiometric oxides. *Solid State Ionics* **6**, 237–252.

Lei, Z. & Zhu, Q. (2005). Low temperature processing of dense nanocrystalline scandia-doped zirconia (ScSZ) ceramics. *Solid State Ionics* **176**, 2791–2797.

Lei, Z., Zhu, Q. & Zhang, S. (2006). Nanocrystalline scandia-doped zirconia (ScSZ) powders prepared by a glycine-nitrate solution combustion route. *J Eur Ceram Soc* **26**, 397–401.

Mizutani, Y., Tamura, M., Kawai, M. & Yamamoto, O. (1994). Development of high-performance electrolyte in SOFC. *Solid State Ionics* **72**, 271–275.

Okamoto, M., Akimune, Y., Furuya, K., Hatano, M., Yamanaka, M. & Uchiyama, M. (2005). Phase transition and electrical conductivity of scandia-stabilized zirconia prepared by spark plasma sintering process. *Solid State Ionics* **176**, 675–680.

Tietz, F., Fischer, W., Hauber, T. & Mariotto, G. (1997). Structural evolution of Sc-containing zirconia electrolytes. *Solid State Ionics* **100**, 289–295.

Tu, H., Liu, X. & Yu, Q. (2011). Synthesis and characterization of Scandia ceria stabilized zirconia powders prepared by polymeric precursor method for integration into anode-supported solid oxide fuel cells. *Power Sources* **196**, 3109–3113.

https://doi.org/10.1017/S1431927613012270 Published online by Cambridge University Press